NURETH14-024

GOTHIC SIMULATION OF SINGLE-CHANNEL FUEL HEATUP FOLLOWING A LOSS OF FORCED FLOW

Xi-Qing Chen¹, A. Tahir¹, Y. Parlatan² and M. Kwee³

¹Department of Thermal Hydraulics Analysis

NSS, 4th Floor, 700 University Ave., Toronto, Ontario, M5G 1X6

²NSATD, Ontario Power Generation, 889 Brock Road, Pickering, Ontario L1W 3J2

³NSASD, Bruce Power, 4th Floor, 123 Front Street W., Toronto, Ontario M5J 2M2

Abstract

GOTHIC v7.2 was used to develop a computer model for the simulation of 28- and 37-element fuel heat-up at a loss of forced flow. The model has accounted for the non-uniformity of both axial and radial power distributions along the fuel channel for a typical CANDU reactor. In addition, the model has also accounted for the fuel rods, end-fittings, feeders and headers. Experimental test conditions for both 28- and 37-element bundles at either low or high powers were used for model validation. GOTHIC predictions of the rod and/or pressure-tube temperatures at a variety of test locations were compared with the corresponding experimental measurements. It is found that the numerical results agree well with the experimental measurements for most of the test locations. Results have also shown that the channel venting time is sensitive to the initial temperature distribution in the feeders and headers. An imposed temperature asymmetry at the beginning will cause the channel flow to vent earlier.

1. Introduction

Under normal operating or shutdown conditions, the reactor fuel is well cooled by pump-circulated flow. Such a mode of fuel cooling may be disrupted when the electrical power supply to the pumps is interrupted. If the pump-forced flow circulation is lost, the fuel and fuel channels will be cooled by the mechanisms of natural circulation. These mechanisms include thermosyphoning and the Channel Cooling in the Absence of Forced Flow (CCAFF), including the Intermittent Buoyancy Induced Flow (IBIF).

The CANDU reactor fuel channel contains 12 or 13 short fuel bundles and located horizontally at the bottom of the heat transport system. The fuel heat-up in the stagnant fuel channel first produces a secondary flow and temperature stratification as a result of the buoyancy effect. This secondary flow is then gradually enhanced as a result of continuous fuel heat-up, and is finally developed to an axially dominated flow moving through the horizontal channel. Such a phenomenon is called venting. Flow venting is a desirable mechanism that can maintain the reactor fuel to be cooled even at a loss of forced flow.

For a long time, the determination of the peak rod surface temperature under such circumstances

(no forced flow) has been relied on the highly empirical methodology [1]. In that methodology, it is assumed that the heat transport system enters a series of predefined natural circulation modes according to a given accident scenario. Based on the determined natural circulation mode, the limiting fuel element and pressure tube temperatures over the entire transient are then determined. It is found that such determined fuel-element and pressure-tube peak temperatures are often over-conservative (a few hundreds of degrees higher) in comparison with the available relevant experimental data. The over-conservatism in the empirical methodology [1] often results in no or low safety margin. Moreover, the empirical method does not even produce the temperature transient over the simulation.

To more realistically predict the fuel-element and pressure-tube peak temperatures, an advanced modeling methodology is required to capture the details of the three-dimensional flow and temperature fields. In this work, the computer code of GOTHIC v7.2 [2] is used to develop a three-dimensional model for simulating the transient temperature and flow fields in the CANDU fuel channels of both 28- and 37-element bundles at a loss of forced flow. This model is able to predict the fuel heat-up, formation of steam bubbles, buoyancy-driven secondary flow, and the axially dominant venting flow. The standing-start experiments for both the 28- and 37-element fuel bundles [3] were used for model validation. Detailed comparison was conducted for the fuel-element and pressure-tube temperature transients at different measurement planes, as described below in Section 2. More modeling details will be presented in Section 3.

2. Experimental setup

The schematic layout of the experimental setup [5] is shown in Figure 1. The test loop consists of a horizontal test channel, inlet and outlet headers, inlet and outlet feeders, water injection lines, a blow-down tank, pumps, pressure and temperature control systems and inter-connecting pipes. The Cold Water Injection Test (CWIT) facility is designed in such a way that the vertical separation between the centerline of the top and bottom channels is 5.0 m, and that the centerline of the headers is 5.0 m above the centerline of the top fuel channel. The centerline elevation of the headers and the centerline of the low fuel channel are separated by a distance of 10.0 m. The heights correspond to the elevations between the headers and the uppermost and lowermost fuel channels of a CANDU reactor. The experimental tests for the 37- and 28-element bundles were conducted using only the lower fuel channel.

The test channel consists of actual CANDU pressure and calandria tubes, end fittings and simulated end-shields. Both end fittings are of CANDU-6 type, each of which has a length of 2.36 m. Both end fittings are equipped with simulated shield plugs and closure assemblies. The calandria tube is located inside a tank. The simulated fuel string consists of 28 or 37 electrically heated fuel element simulators (FES) assembled in typical 28- or 37-element CANDU fuel bundle geometry with an overall length of 11.6 m, including a heated length of about 6 m. By adjusting the voltage applied to the different rings, the fuel simulators can achieve an outer to centre rod flux depression ratio of 1.0/0.81/0.72/0.68 for the 37-element bundle and 1.0/0.82/0.74 for the 28-element bundle.

The assembled bundle contains either 28 or 37 identical elements. Each element consists of a heater-filament assembly that is surrounded by a heater sheath. A heater filament is made of an Inconel-600 tube that has an O.D. of 6.35 mm and an I.D. of 5.33 mm [3]. The entire heater

filament assembly is placed inside an Inconel tube that serves as the outer sheath. The entire assembly has twelve segments, each of which has a length of 495.3 mm [3]. The pressure tube is a Zircalloy-2.5% niobium tube with an O.D. of 112.4 mm and an I.D. of 103.8 mm [3]. The pressure tube is housed in a square channel enclosure. This enclosure can be filled with liquid water to simulate the reactor moderator.

3. Numerical details

3.1 GOTHIC v7.2 computer code

GOTHIC is a general-purpose, three-dimensional thermal-hydraulics computer code. It can be used to perform a variety of nuclear safety and licensing analyses. In GOTHIC, the transient behavior of a multiphase flow is modeled using three separate fluid phases: vapor, droplets and continuous liquid [2]. The vapor phase can be comprised of steam and/or a number of noncondensing gas components, all of which are assumed to be at the same local temperature and velocity. The droplets have the same local diameter, temperature and velocity. The continuous liquid phase refers to water in any geometric configuration except drops (films, pools etc). For each of the three fluid phases, mass, energy and momentum balances are maintained for a set of finite volumes. Within each volume, each phase has its own temperature and velocity. All three phases are assumed to be compressible. Constitutive models are used to calculate the transfer of mass, energy and momentum between the phases and between the walls and the fluid.

GOTHIC accounts for a variety of heat and mass transfers among different fluid phases, and the heat transfer between a fluid phase and a solid structure (termed as a thermal conductor in GOTHIC). Heat conduction within a solid structure can also be calculated using the heat-conduction equation. Energy balances are maintained for solid thermal conductors with heat transfer at the surfaces to the vapor and liquid phases. GOTHIC has found wide applications in different analyses ([6], [7]). One of the advantages of the GOTHIC code is that it can easily combine detailed modeling (using subdivided volumes) with lumped-parameter volumes in a single model for flows with complex geometry. GOTHIC has the capability of dividing a computational domain into multiple sub-domains which are then connected to each other through three-dimensional flow connectors. This capability is similar to the domain-decomposition method used in many CFD codes. Solid obstructs in the flow domain can be treated using the porosity model.

3.2 Overall modeling of the standing-start tests

As shown in Figure 1, the standing-start CWIT facility consists of many components. It is not possible to model all of the system components in detail. Therefore, a computer model has been developed to account for the following major components:

- 1) Twelve heated fuel element simulators
- 2) Inlet and outlet end-fittings
- 3) Pressure tube and liner tube modeled as the GOTHIC "CYLINDICAL" blockages
- 4) Inlet and outlet feeder piping lines
- 5) Inlet and outlet headers
- 6) Blow-down tank

Note that the inlet and outlet end-fittings, inlet and outlet feeder piping lines and inlet and outlet headers are symmetric in the test. They are also modeled symmetrically in this work. Of the above listed six components, Items 1) and 2) are the two key components required to be modeled in detail. GOTHIC subdivided volumes are used to model the end-fittings and the heated fuel element simulators. The remaining four items, which are secondary but required to construct the entire system model, are modeled using the GOTHIC lumped-parameter volumes.

Each of the twelve heated fuel element simulators has a length of 495.3 mm, and there are a total of 37 fuel rods for the 37-element bundle and 28 rods for the 28-element bundle in each fuel element simulator. Figure 2 shows the three-dimensional view of one fuel element simulator with 37 or 28 rods. In the CWIT experiment, electrical power is supplied to the 37 or 28 rods, and is controlled to achieve the intended power load and distribution. The axial power distribution along the heated length (of about 6 meters) is a smooth cosine shape for the 37-element bundle, and a polynomial for the 28-element bundle. Modeling of the power distributions for both of the 37- and 28-element fuel bundles in GOTHIC are outlined below.

3.3 Axially cosine power distribution

For the 37-element fuel bundle type, the axial power profile in the simulated fuel string is a smooth symmetrical cosine shape **Error! Reference source not found.**; see Figure 9(a). The maximum axial flux factor is 1.485 times the average flux and occurs at the center of the string. The minimum flux is at the ends of the heated length and is 0.15 times the average power. The 37-element axial power distribution is given by

$$\frac{q(x)}{q_{ave}} = 1.485 \times \cos(0.490x) \qquad (-3.0 \ m \le x \le 3.0 \ m)$$
 (1)

where q(x) is the power output per unit length for a particular element (W/m), q_{ave} the average power output per unit length (W/m), and x the axial distance (m) with the reference zero defined at the FES string center. By adjusting the voltage applied to the different rings, the fuel element simulators have an outer to centre rod flux depression ratio of 1.0/0.81/0.72/0.68Error! Reference source not found. The average design heat flux for the 37-element fuel bundles are 1.9 W/cm^2 .

For the 28-element fuel bundle type, the axial power distribution for the heated section of the 28-element Fuel Element Simulators is determined using a polynomial as follows:

$$q(x) = C_0 + C_1 x + C_2 x^2 + C_3 x^3 + C_4 x^4 + C_5 x^5 + C_6 x^6$$

$$= \sum_{n=0}^{6} C_n x^n \qquad (-3.0 \ m \le x \le 3.0 \ m)$$
(2)

The coefficients of the curve-fit polynomial can be found in Figure 9(b). All the rods belonging to the same ring have the same power distribution. A total of 24 computational domains are used to model the 6-meter heated length. The remaining 5.6m-unheated length forms part of the two end-fittings, and is included in the modeling of the end-fittings. GOTHIC three-dimensional flow

connectors are used to connect each two adjacent domains. The heat release rate through each of the 28 or 37 rods is modeled using GOTHIC thermal conductors. Given a total channel power, the axial power distribution can be first determined in terms of a cosine shape or a polynomial function. Then each ring power is calculated using the ring-wise power distribution. Finally, based on the total number of rods in each ring, the heat release rate through each rod is calculated and used as model heat source input.

3.4 Heated fuel element simulators

Each of the 24 computational domains is then further subdivided into 3x10x10 finite volumes. Therefore, a total of 72x10x10 finite volumes are used to model the six-meter heated fuel element simulators. This grid has been found to give a grid-independent solution. The 28 or 37 rods and the pressure tube are modeled as GOTHIC blockages. Based on the input rod and pressure tube geometries, the GOTHIC preprocessor will automatically calculate the area and volume porosities. The numerical grids for one Fuel Element Simulator with a length of 495.3 mm are shown in Figure 2.

3.5 Inlet and outlet end-fittings

The 6m-heated fuel element simulators, together with the additional 5.6m-unheated length, are connected, through the GOTHIC 3D flow connectors, with the inlet and outlet end-fittings, which are then further connected, through GOTHIC flow paths, with the inlet and outlet feeders. The two end-fittings are symmetric and complex in geometry. It is not possible to model them in detail. The two end-fittings are modeled using GOTHIC blockages to account for the annulus geometry. The simplified end-fitting model has accounted for the major geometric features such as the annulus, unheated fuel bundle extension and liner tube etc. A total of 9x12x12 of finite volumes is used to model each of the two end-fittings. The numerical grids and the blockages used to model each end-fitting are shown in Figure 3. Note that each of the two end-fittings includes the unheated fuel simulators of 2.8 m (half of the total unheated length).

3.6 Miscellaneous components

In addition to modeling the major components of heated fuel element simulators and end-fittings, other components such as feeder piping, headers and blow-down tank, need also be included in the modeling system. These components are modeled using GOTHIC lumped-parameter volumes, and are joined with each other through GOTHIC flow paths. The lumped-parameter volumes account for their actual elevations and volumes. As such, the entire modeling system can adequately model energy storage.

3.7 Experimental tests for the simulated 37-element bundle

Two CWIT test cases, one for Test #1620 at low power and another for Test #1626 at high power, were selected for validating the GOTHIC model for the 37-element bundle. The initial channel temperature, pressure and total power for each of the two tests are as follows:

- 1) Test #1620: temperature 30°C, channel center pressure 7100 kPa, Power 50 kW
- 2) Test #1626: temperature 100°C, channel center pressure 1600 kPa, Power 151 kW

The saturation temperatures at 7100 kPa and 1600 kPa are 286.8°C and 201.4°C, respectively. Initial liquid volume fractions are all set to unity since the entire modeling system is full of

water. Pressure boundary condition is implemented through the blow-down tank. As a result, the flow entering and leaving the system can be accounted for to ensure that the system pressure is maintained at the test pressure. For the low power case (Test #1620), only symmetric initial temperature conditions are used. For the high power case (Test #1626), however, two runs are conducted: one using the constant initial temperature everywhere and the other imposing a slight temperature asymmetry (0.1°C) on one side of the feeder and header. The two run results are then compared with each other and with the CWIT measurements.

3.8 Experimental tests for the simulated 28-element bundle

Two CWIT test cases, one for Test #1333 at low power and another for Test #1326 at high power, were selected for validating the GOTHIC model for the 28-element bundle. The initial channel temperature, pressure and total power for each of the two tests are as follows:

- 1) Test #1333: temperature 69°C, channel center pressure 1090 kPa, Power 52 kW
- 2) Test #1326: temperature 111°C, channel center pressure 1142 kPa, Power 132 kW

The saturation temperatures at 1090 kPa and 1142 kPa are 184°C, and 185.7°C, respectively.

3.9 Thermocouple locations for temperature measurements

For the experimental measurements of the 37-element bundle, the rod surface temperatures are available at many thermocouple locations for several planes along the heated length; see Figure 4. These temperature measurements are used to validate the present computer model. The thermocouple locations for the pressure tube temperature measurements are shown in Figure 5. A lot of data points at Planes B, D, F, G, I, and K are available for comparison. However, only the predictions near the channel center at Planes F (or F1) and G (or G1) are compared with the corresponding measurements. The thermocouple locations for temperature measurements of the 28-element bundle are shown in Figure 6.

4. Results and discussion

4.1 37-Element Fuel Bundle

The 37-element model is first validated against the low-power channel conditions (Test #1620). For this test, the constant initial temperature conditions are implemented. That is, no temperature asymmetry in the inlet feeder and header is imposed. The GOTHIC predicted rod-surface temperatures at various test locations are compared with the CWIT data. Shown in Figure 10(a) and Figure 10(b) are the predicted and measured rod-surface temperature transients at Planes F1 and G1, respectively. The comparisons show that the GOTHIC predictions agree well with the experimental measurements. The model provides good prediction of the temperature transients during the heat-up and venting periods. As expected, the high temperatures occur at the top (Rod #10) of the middle fuel channel. The predicted peak rod surface temperature agrees very well with the experimental measurement. The comparison also shows that the predicted channel flow venting time is slightly earlier than the test, as observed by the timing at which the rod temperature starts to decrease in the transient.

The predicted and measured pressure-tube surface temperature transients at Planes F1 and G1 are shown in Figure 11(a) through Figure 11(b), respectively. The model predictions are in good agreement with experimental measurements. The predicted pressure-tube surface temperature

transients have the same trend as those of the rod surface. That is, the temperature starts to decrease as the channel flow increases due to venting. The predicted temperature decrease starts slightly earlier than the experiment, as a result of the predicted earlier venting.

Test #1626 has an initial temperature of 30°C, a channel power of 151 kW, and a channel center pressure of 1.6 MPa at which the saturation temperature is 201.4°C. Two runs were conducted for this test: one using the symmetric (uniform) initial temperature (30°C) conditions and the other using the asymmetric initial temperature conditions (inlet feeder and inlet header temperature reduced by 0.1°C). The predicted and measured rod-surface temperatures are compared in Figure 12(a) and Figure 12(b). The predicted and measured pressure tube temperatures are compared in Figure 13(a) and Figure 13(b).

As shown in Figure 12(a), the peak rod-surface temperature is over-predicted when the symmetric initial temperature conditions are used. However, the peak-rod surface temperature is slightly under-predicted when the slightly asymmetric initial temperature conditions are imposed in one side of the feeder and header. Table 2 lists the predicted and measured peak rod and pressure-tube surface temperatures, where a positive difference indicates an over-prediction whereas a negative difference indicates an under-prediction. As expected, the results obtained with the symmetric temperature input conditions are more conservative. The peak rod-surface temperature difference between the prediction and measurement is over-predicted by 70.8°C for the symmetric temperature initial conditions, and is under-predicted by 18.7°C for the asymmetric temperature initial conditions. The slightly imposed asymmetric initial temperature conditions have under-predicted the peak PT temperature 43.1°C. However, use of symmetric initial temperature conditions has over-predicted the peak PT temperature by 34.2°C. The channel venting time for this high power test is also shown in Table 2.

Channel liquid level is one of the important parameters for assessing the extent of fuel element dry-out at high power. For each CWIT test, the experimental data are available for the channel liquid levels [9]. Since the GOTHIC code does not provide an explicit output of the liquid level, the following indirect method has been used to determine the liquid level:

- Generate the transient void fraction for the subdivided volume in the middle of the channel using the GOTHIC pre-processor
- Plot void contours
- Export each contour snapshot at each time step
- Print out the contour plots with lowest liquid level
- Determine the liquid level from the printout
- Calculate the liquid level fractions using the channel diameter

Figure 14(a) and Figure 14(b) show the lowest liquid level for Test #1626 using the symmetric and asymmetric temperature conditions, respectively. It can be seen that the top fuel elements are dried out. Based on these plots, channel liquid levels are estimated and are compared with the experiment. The comparison results for the three high-power tests are listed in Table 1. It is seen that the predictions are in good agreement with the CWIT data [9]. The maximum difference between the predicted and measured liquid height fractions is 6.2%, which is within the experimental uncertainty. A snapshot of water temperature contours for the channel and end-fittings is shown in Figure 18.

4.2 28-Element Fuel Bundle

Figure 15(a) and Figure 15(b) compare the measured and predicted transient sheath temperatures at different thermocouple locations for Test #1333. The two sets of GOTHIC results, one obtained with the symmetric initial temperatures and another obtained with the slightly asymmetric initial temperatures (reduced by an arbitrary small value of 0.3°C in one side of the feeder and header to ensure the flow venting occurs earlier), are plotted in the same figure for comparison. The results show that the channel venting time is sensitive to the imposed initial temperature asymmetry. GOTHIC predicted peak sheath temperatures for the symmetrical and asymmetric initial temperature conditions are 196°C and 185°C, respectively. In contrast, the measured peak sheath temperature for this test is 188°C.

Figure 16(a) and Figure 16(b) compare the transients of predicted and measure rod-surface temperatures at different thermocouple locations; see Figure 6 and Figure 8 for the definition of the 28-element thermocouple locations. Figure 16(a) shows that the temperature of the top rod (Rod#4) in the middle of the channel starts to decrease as early as 350s for the symmetric initial temperature conditions and 315s for the asymmetric conditions. The sharp temperature decrease occurs at 437s for the symmetric initial temperature conditions and at 393s for the asymmetric conditions. In contrast, the experiment indicates that a rapid temperature decrease occurs at 300s; see Table 3. This happens because the predicted inflow of cool water is not enough to quickly submerge the top rods. For the rods at the lower levels, however, an earlier and more rapid temperature decrease is predicted; see the temperature transients of ROD-19G and ROD-8G in Figure 16(b). This is because the inflow of cool water quickly submerges the rods at lower levels (third and fourth rows of rods as shown in Figure 8. A summary of predicted and measured peak sheath temperatures, together with the channel venting time, for the 28-element fuel bundle is given in Table 3. It is shown that the GOTHIC predictions are conservative.

The predicted liquid level for this high power test is compared with that for the corresponding experiments [4]. The liquid level for the 28-element fuel bundle is determined in the same way as that for the 37-element fuel bundle. The representative contours of the vapour volume fraction are shown in Figure 17(a) and Figure 17(b) obtained using the symmetric and asymmetric initial temperature assumptions, respectively. The estimated liquid levels are given in Table 4. It is seen that the GOTHIC predicted liquid level is not sensitive to the imposed slight temperature asymmetry.

5. Conclusion

Computer models were developed using GOTHIC to simulate single channel fuel heat-up following a loss of forced flow for both the 37- and 28-element fuel bundles. Both low and high power tests were used to validate the computer models. The transient rod-surface temperatures and the pressure tube surface temperatures were compared with the corresponding experimental measurements. It was found that for the 37-element fuel bundle no temperature asymmetry was required to achieve better agreement between the predictions and measurements. For the 28-element fuel bundle, however, it was found that a temperature asymmetry was required to achieve better agreement between the predictions and measurements. The predicted liquid levels for both the 37- and 28-element fuel bundles were in good agreement with the experiments.

6. References

- [1] Amrounti J.-C., Bolander T.G. and Feyginberg Y., "Methodology for the Assessment of Channel Cooling in the Absence of Forced Flow", Report No. 85323, 1986.
- [2] Numerical Applications, Inc., "GOTHIC Containment Analysis Package User Manual Version 7.2b (QA)", NAI File NAI 8907-02 Rev 18, March 2009.
- [3] Shin K.S., "Data Report for Standing Start Tests Conducted with the West Channel in the Cold Water Injection Test Facility (Test Nos.1608 to 1686)", Stern Lab Report No. SL-126, OPG file N-08800-2164 P, May 2001.
- [4] K.S. Shin, "Data Report for Standing Start Tests in MCT-CWIT Facility (Test Nos.1315-1377), Stern Lab Report No. SL-002, June1988.
- [5] McCallum C.K. and Wedgewood J.M., "Description of the Cold Water Injection Test Facility", COG Report No. COG-96-255, June 10, 1996.
- [6] Analytis G. Th. and Andreani M., 2001, "On the boundary conditions of the k-ε model in 3D coarse-mesh models for containment analysis", Nuclear Engineering and Design, vol. 205, pp. 53-67.
- [7] Lee Jin-Yong, Lee Jung-Jae and Park Goon-Cherl, "Assessment of the GOTHIC code for prediction of hydrogen flame propagation in small scale experiments", Nuclear Engineering and Design, vol. 236, 2006, pp. 63-67.
- [8] Feyginberg Y., de Man H.G.O., Amrouni J.-C., and Tomada F., "Channel Cooling in the Absence of Forced Flow (CCAFF) Methodology Update", Report No. 88665, September 1988.
- [9] Tabatabai M. and Tahir A.," Utilization of Data from the Standing Start Tests Conducted in the CWIT Facility in Stern Laboratories", NSS File No. G0026/AR/001, October 25, 2002.

Table 1 Comparison of Predicted and Measured Relative Channel Liquid Levels for the 37-Element Fuel Bundle

GOTHIC ID	Initial Temperature Conditions	Minimum Liquid Height Fraction (%)		Difference (%)
		Prediction	Experiment [9]	(70)
T1626-151kW-Asym	Asymmetric	74.2	68	6.2
T1626-151kW-Symm	Symmetric	69.8	68	1.8

Table 2 Comparison of Predicted and Measured Peak Temperatures and Venting Times for the 37-Element Fuel Bundle

COTINGID	Peak Rod Surface Temperature (°C)				
GOTHIC ID	CWIT [9]	GOTHIC	Error (°C)		
T1626-151kW-Asym	517	498.3	-18.7		
T1626-151kW-Symm	517	587.8	70.8		
GOTHIC ID	Peak Pressure Tube Temperature (°C)				
GOTTILE ID	CWIT [9]	GOTHIC	Error (°C)		
T1626-151kW-Asym	294	250.9	-43.1		
T1626-151kW-Symm	294	328.2	34.2		
GOTHIC ID	Channel Flow Venting Time (s)				
GOTHIC ID	CWIT [9]	GOTHIC	Error (s)		
T1626-151kW-Asym	416.0	341.1	-75		
T1626-151kW-Symm	416.0	405.1	-11		

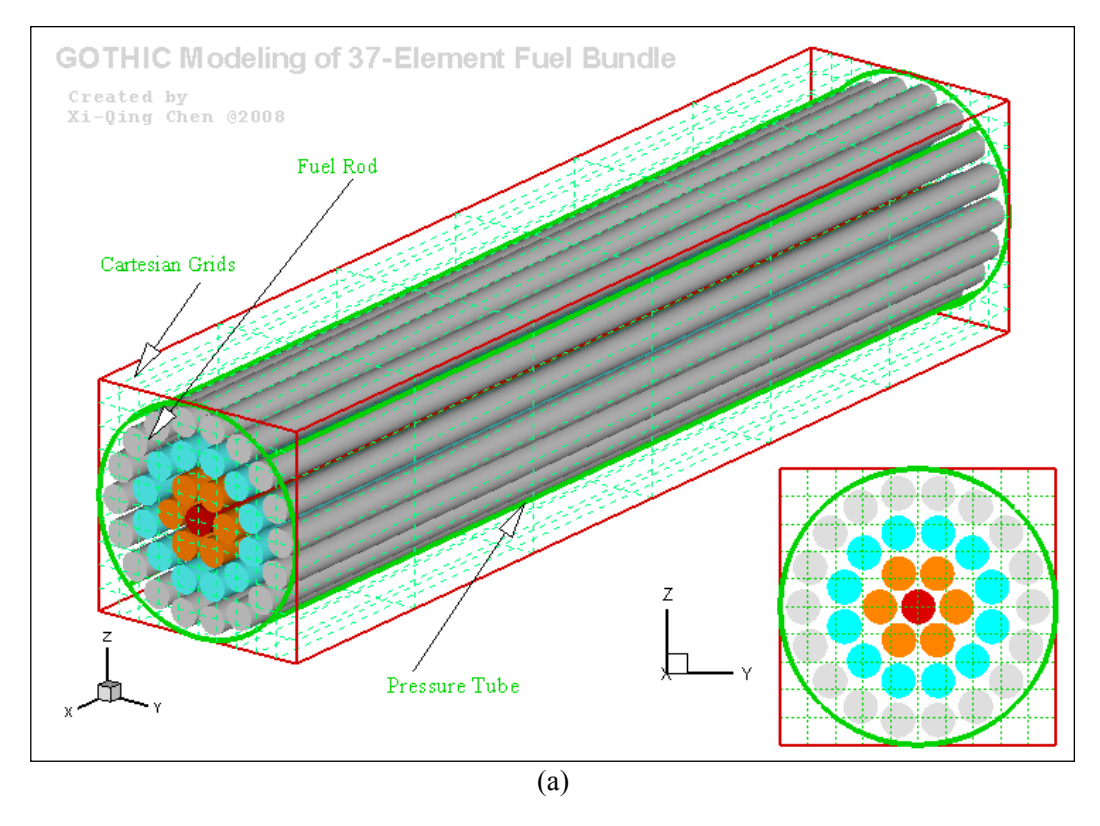
Table 3 Comparison of Predicted and Measured Peak Temperatures and Venting Times for the 28-Element Fuel Bundle

GOTHIC ID	Peak Rod Surface Temperature (°C)				
GOTTILE ID	CWIT	GOTHIC	Error (°C)		
T1326-132kW -Asym	538	583	45		
T1326-132kW -Symm	538	606	68		
GOTHIC ID	Channel Flow Venting Time (s)				
GOTTILE ID	CWIT	GOTHIC	Error (s)		
T1326-132kW -Asym	300	315	15		
T1326-132kW -Symm	300	350	50		

Table 4 Comparison of Predicted and Measured Relative Channel Liquid Levels for the 28-Element Fuel Bundle

GOTHIC ID	Initial Temperature Conditions	Minimum Liquid Height (mm)		Difference
		Prediction	Experiment [9]	(mm)
T1326-132kW-Asym	Asymmetric	55	62	-7
T1326-132kW -Symm	Symmetric	55	62	-7

Figure 1 Experimental Setup



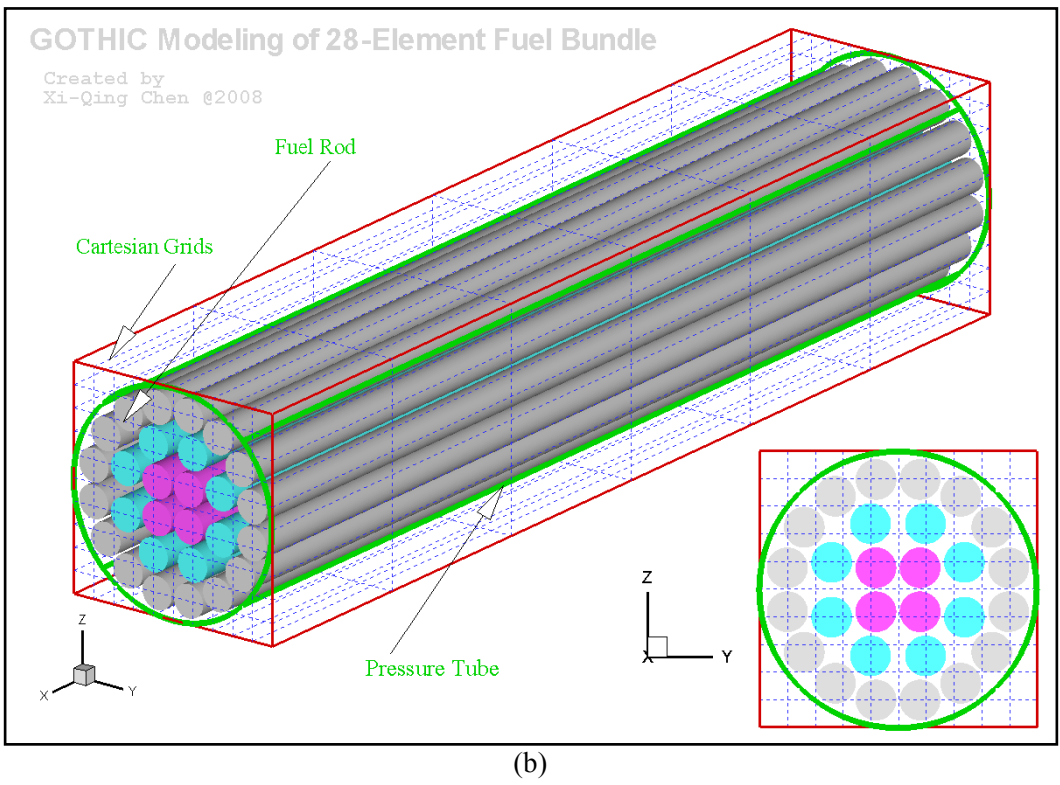
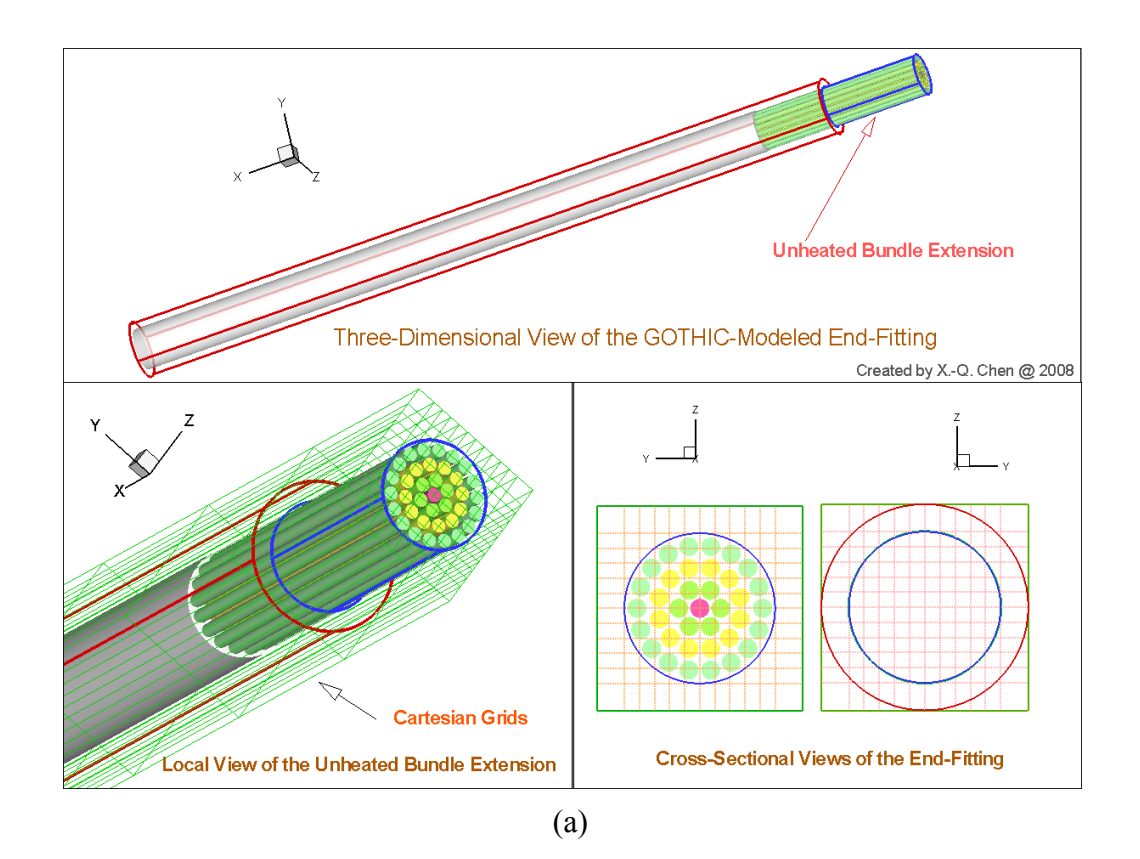


Figure 2 Numerical Grids for One Fuel Bundle: (a) 37-Element and (b) 28-Element Fuel Bundles



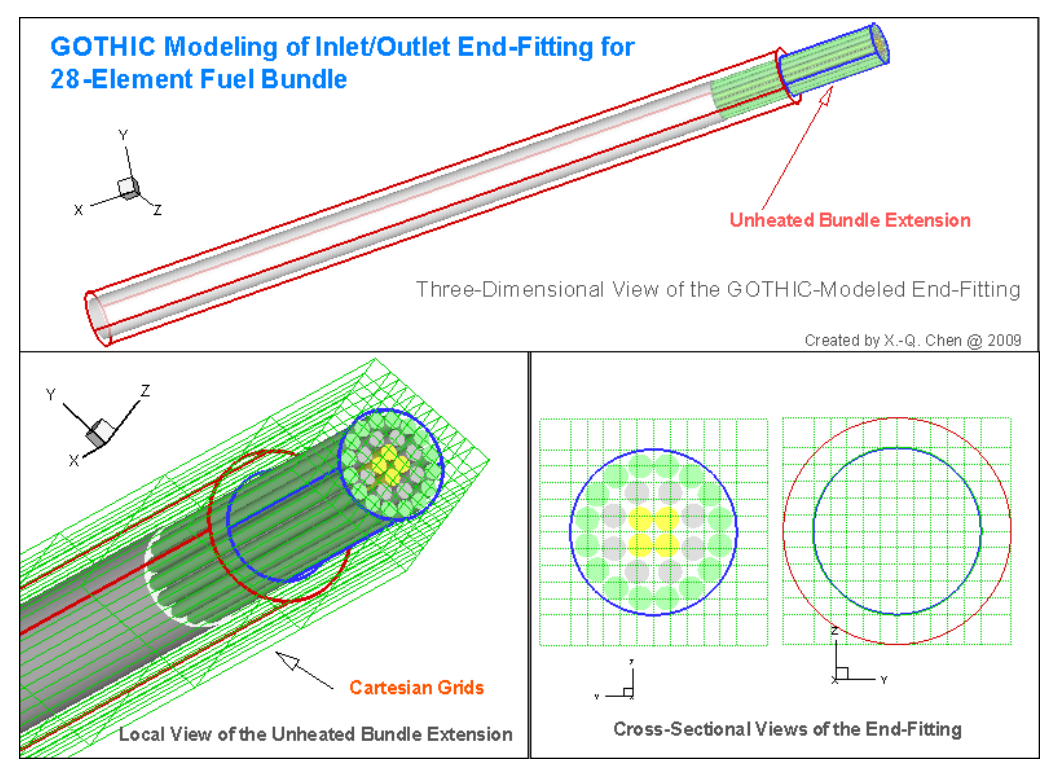


Figure 3 Numerical Grids and Cylindrical Blockages for One End-Fitting: (a) 37-Element and (b) 28-Element Fuel Bundles

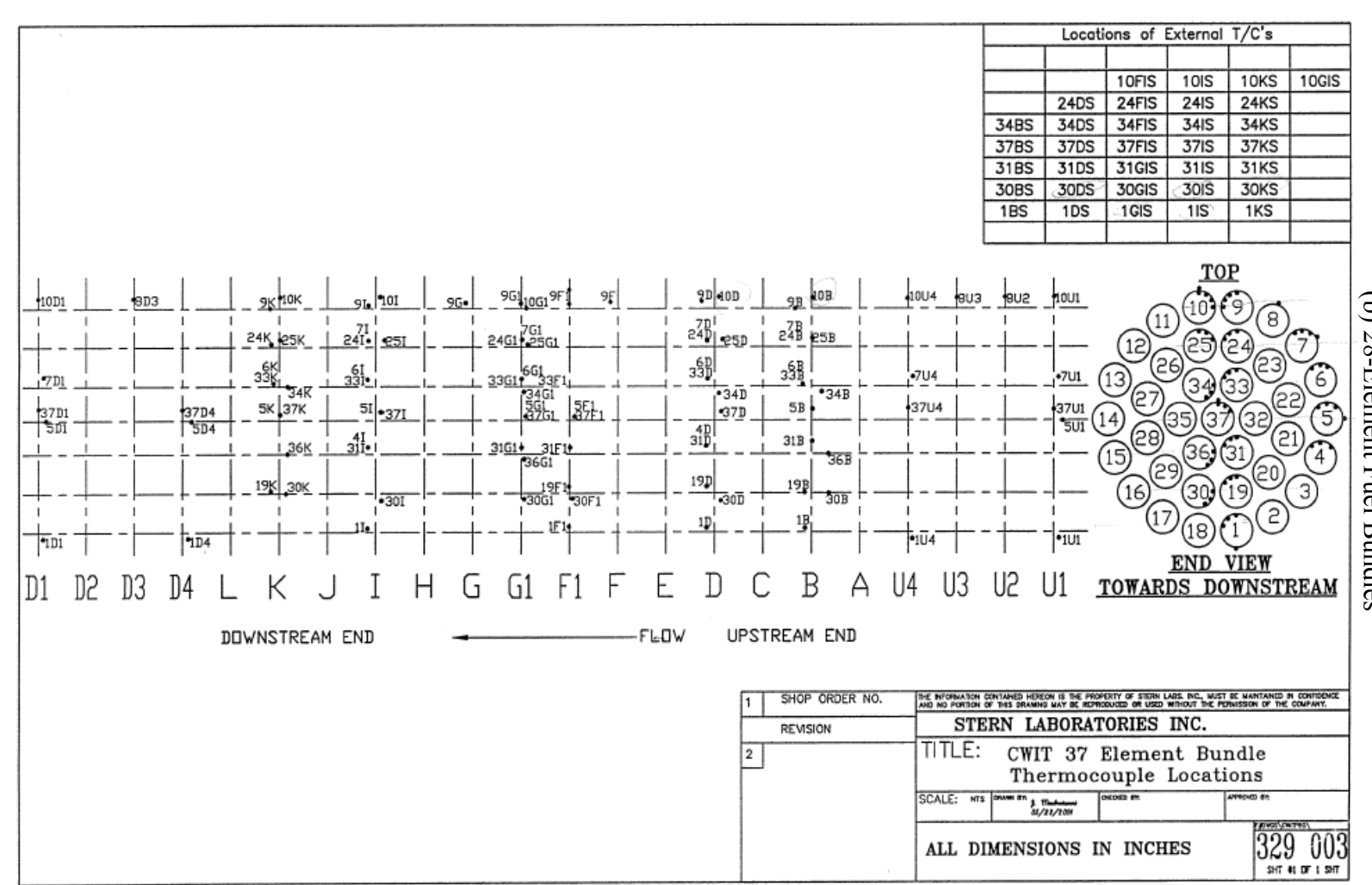


Figure 4 Thermocouple Locations for the 37-Element FES

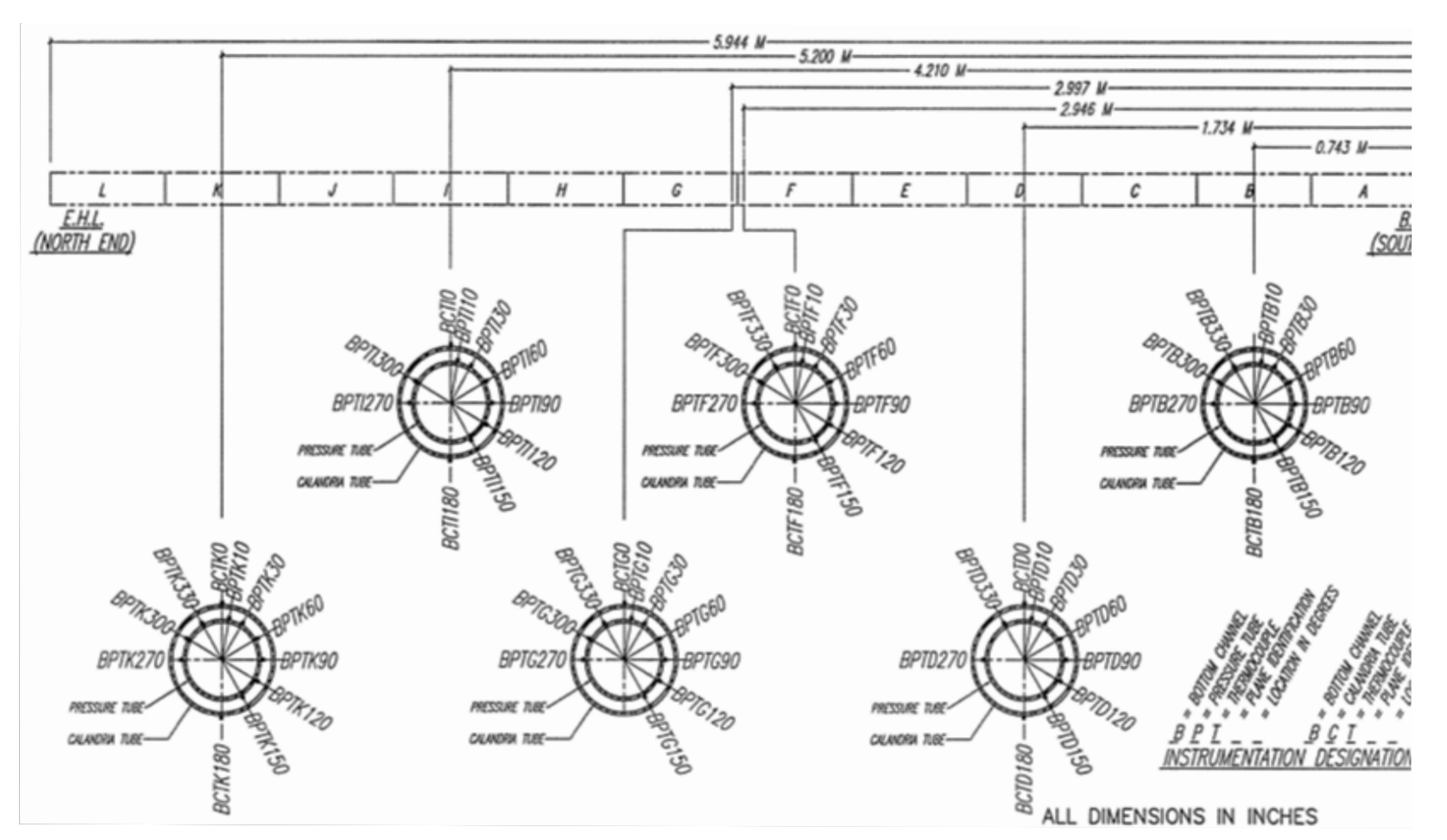


Figure 5 Thermocouple Locations for the Pressure Tube Temperature Measurements

Figure 6 Thermocouple Locations for the 28-Element FES

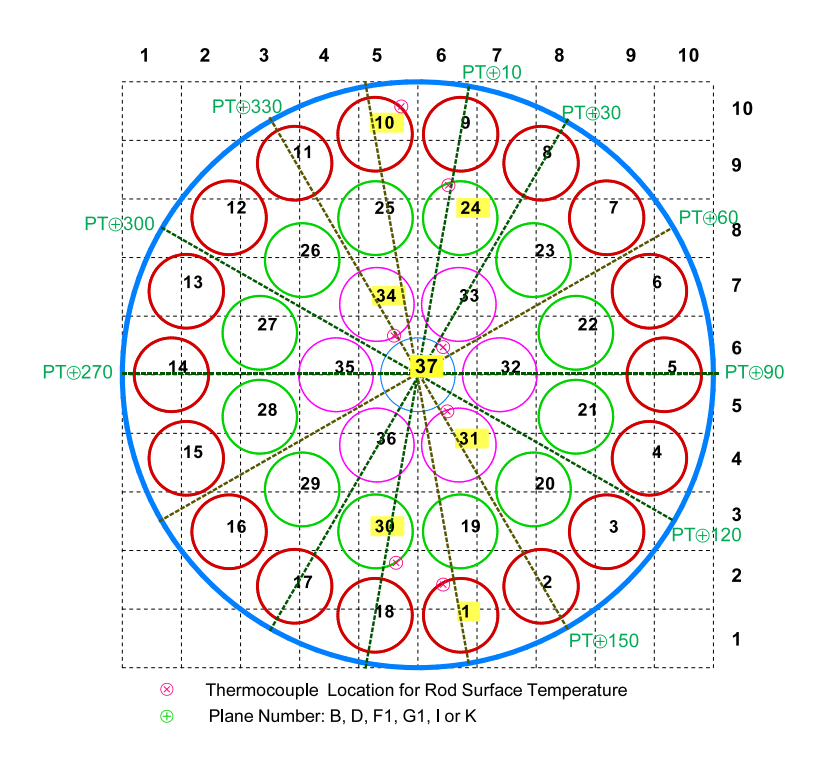


Figure 7 Thermocouple Locations for Measuring Rod and Pressure-Tube Surface Temperatures of the 37-Element Fuel Bundle

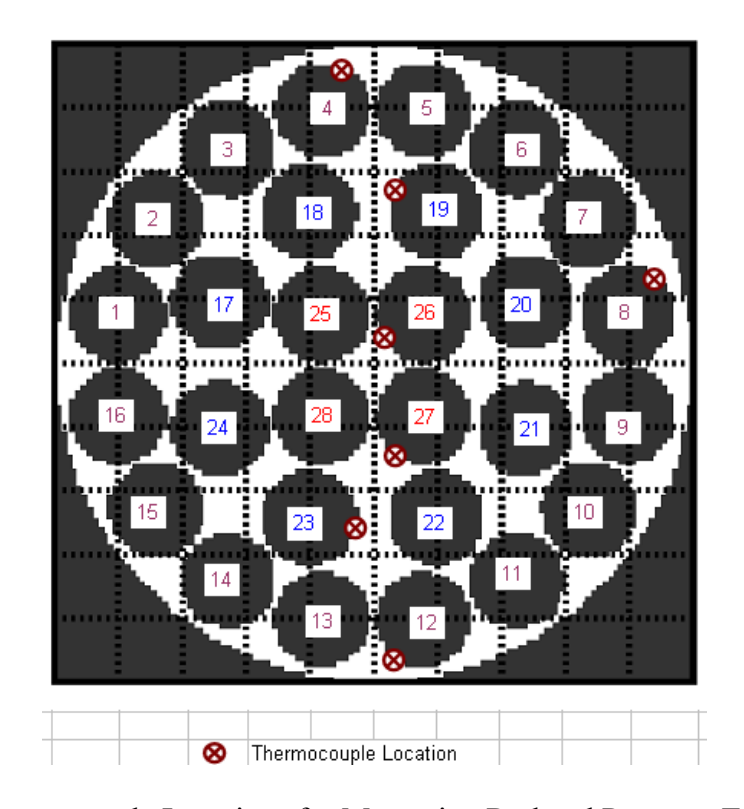
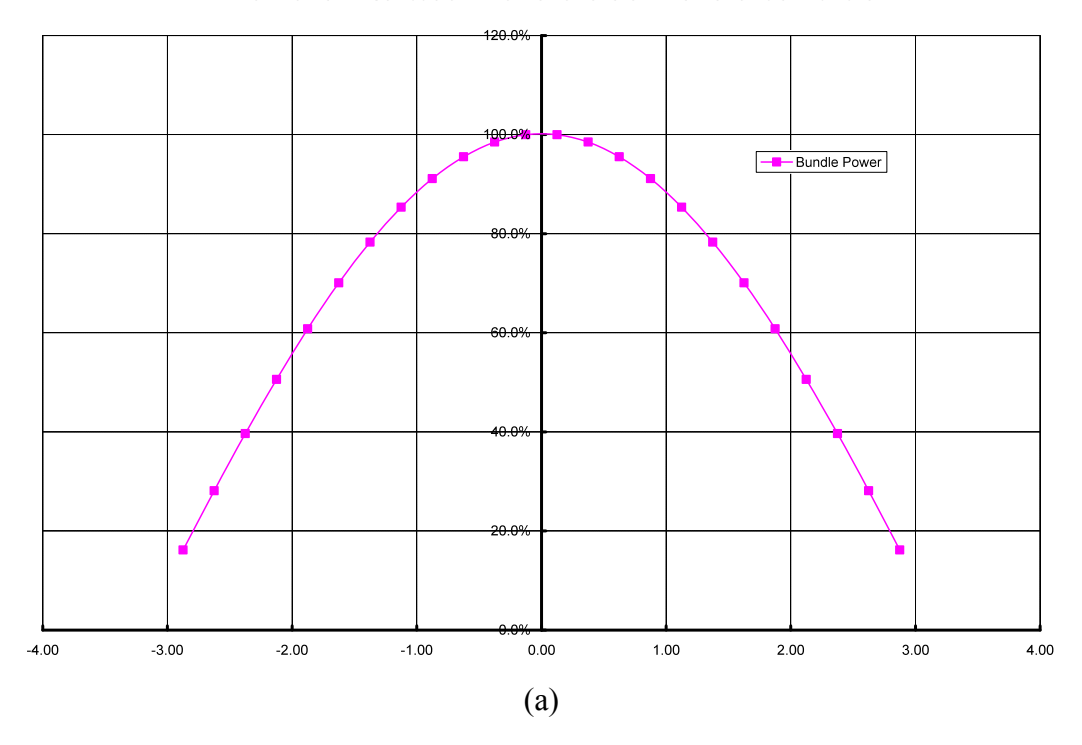


Figure 8 Thermocouple Locations for Measuring Rod and Pressure-Tube Surface Temperatures of the 28-Element Fuel Bundle

Axial Power Distribution Profile for the 37-Element Fuel Bundle



Axial Power Profile for the 28-Element Bundle

 $P(x) = 3.4032 - 04x^6 - 2.1072 - 13x^5 - 7.1482 - 03x^4 - 9.3931 - 12x^3 - 6.4982 - 02x^2 - 1.2242 - 10x + 1.0050 + 00$

Relative Power along Heated Section

O CMIT Data Points

Curve-Fit

80%

40%

20%

-1.0

-3.0

-2.0

Figure 9 Axial Power Distributions: (a) 37-Element Fuel Bundle and (b) 28-Element Bundle

0.0

Axial Distance (m) (b)

1.0

2.0

3.0

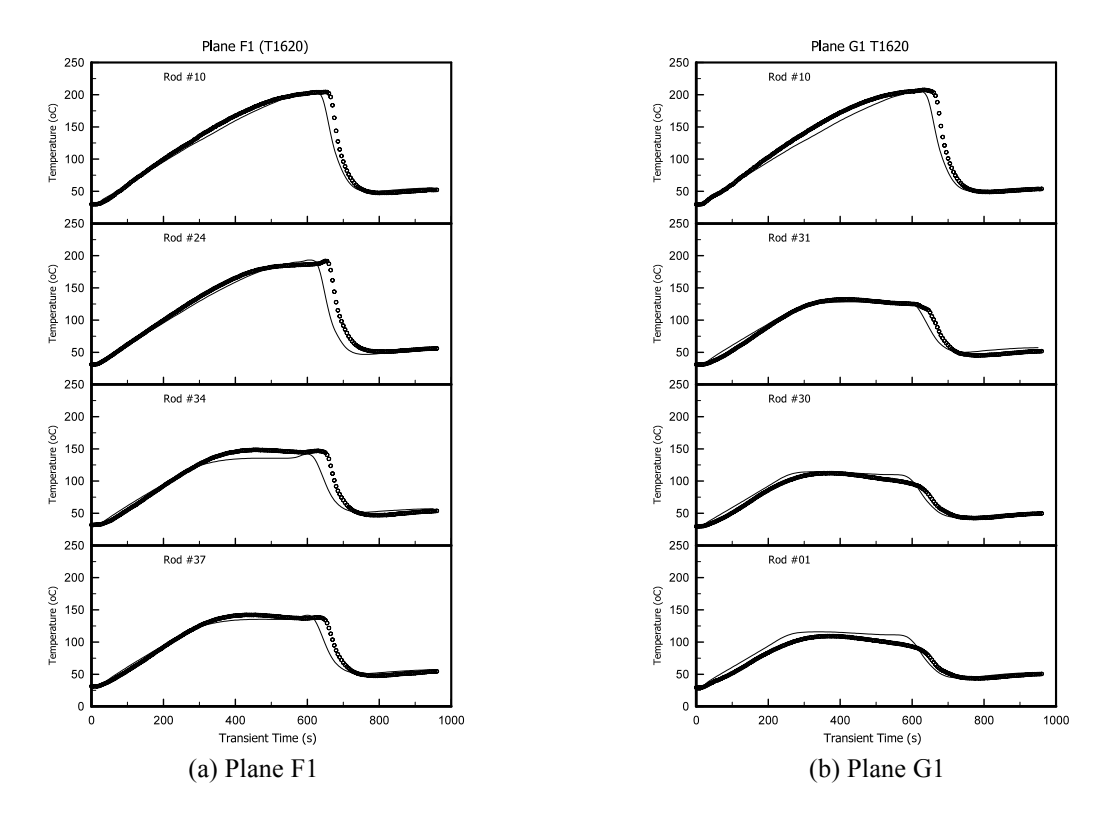


Figure 10 Comparisons of Rod-Surface Temperatures (Test #1620)

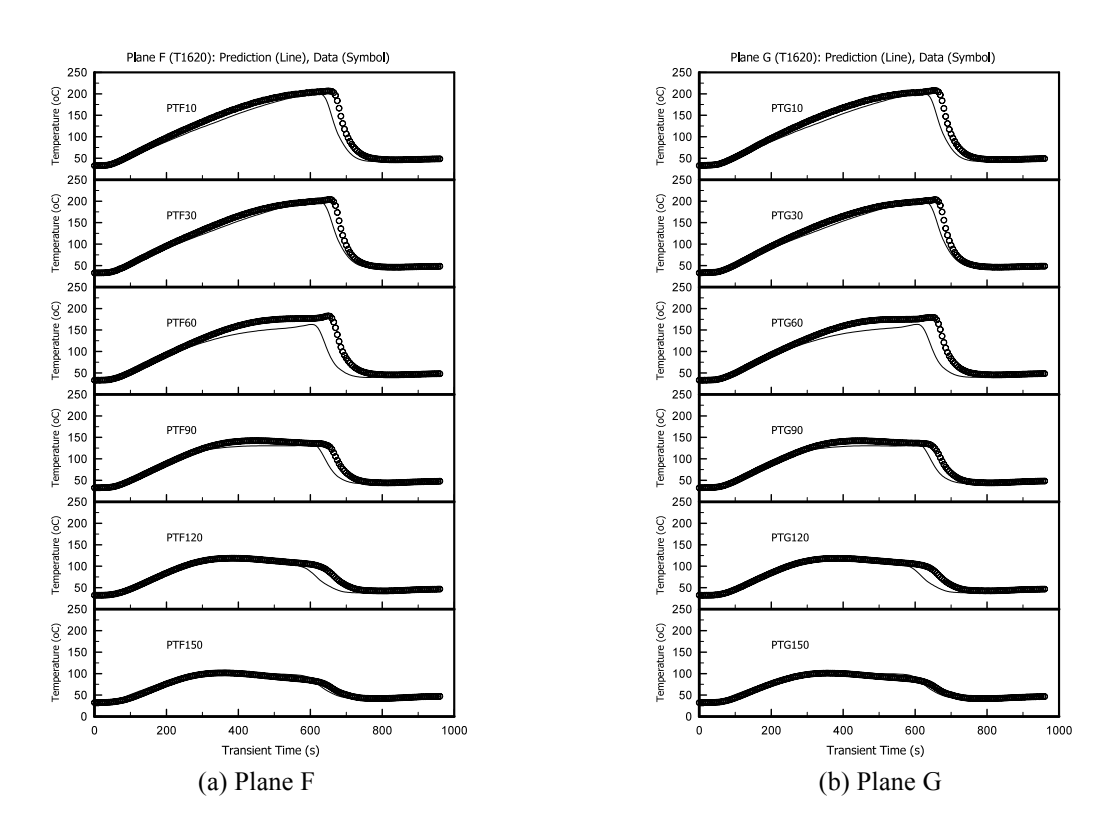


Figure 11 Comparisons of Pressure-Tube Surface Temperatures (Test #1620)

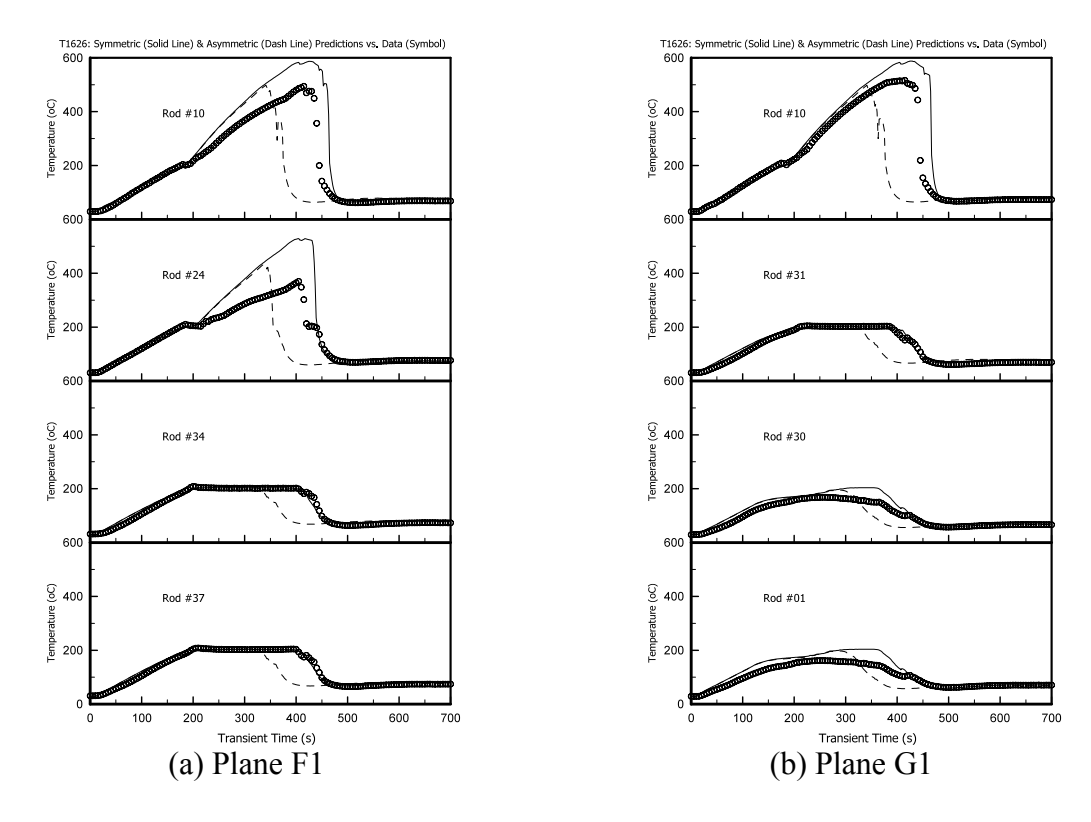


Figure 12 Comparisons of Rod-Surface Temperatures (Test #1626)

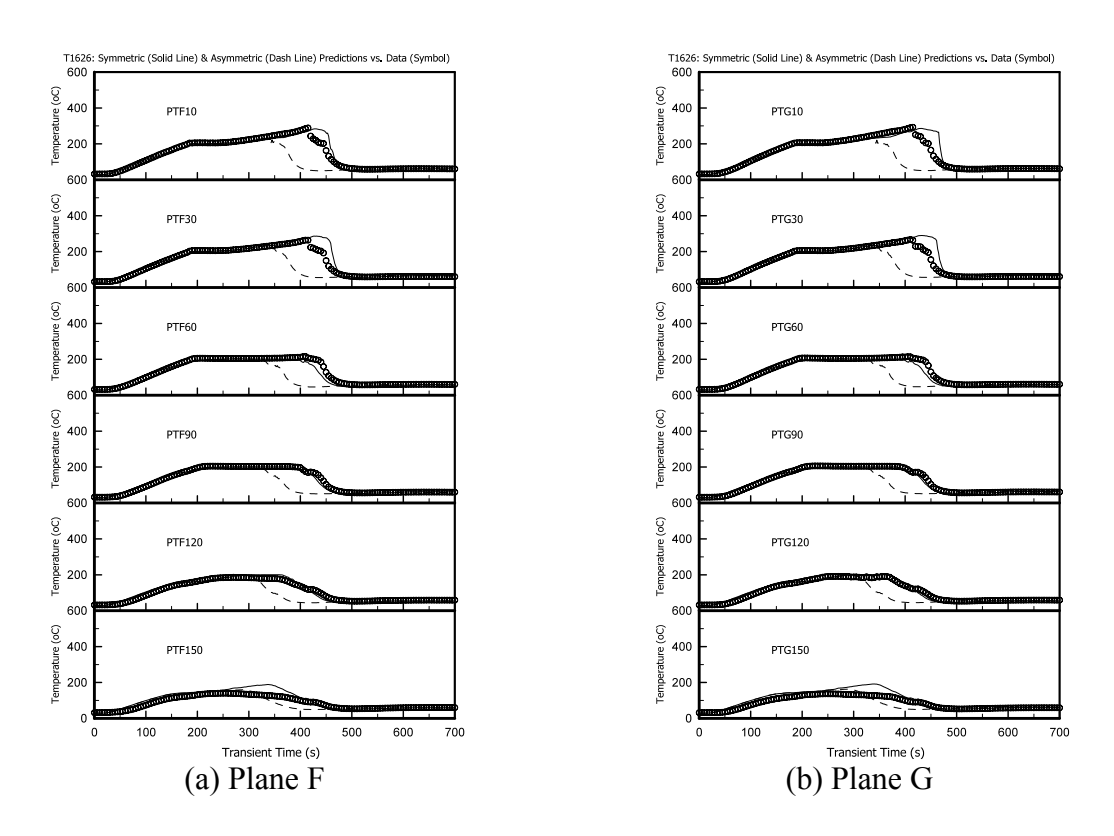
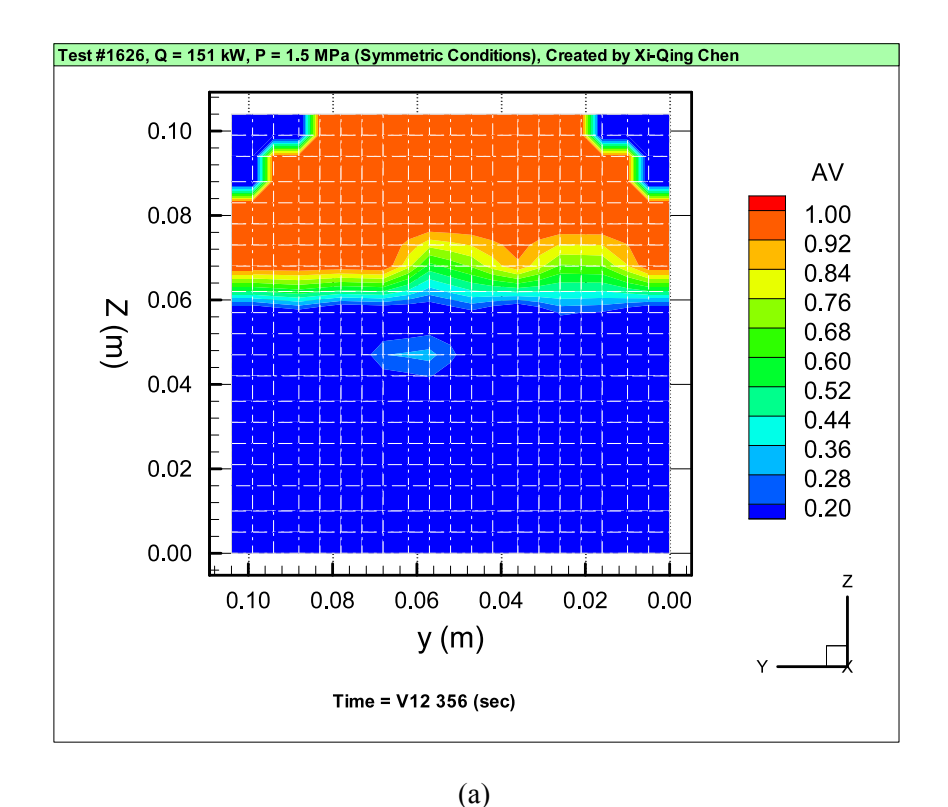


Figure 13 Comparisons of Pressure-Tube Surface Temperatures (Test #1626)



Test #1626, Q = 151 kW, P = 1.5 MPa (Asymmetric Conditions), Created by Xi-Qing Chen 0.10 ΑV 0.08 1.00 0.92 0.84 Z (m) 0.06 0.76 0.68 0.60 0.04 0.52 0.44 0.36 0.02 0.28 0.20 0.00 0.06 0.04 0.10 0.08 0.02 0.00 y (m) Time = V12 282 (sec) (b)

Figure 14 Contours of Steam Bubbles at the Middle Channel for Test #1626: (a) Symmetric at 280 s and (b) Asymmetric at 282 s

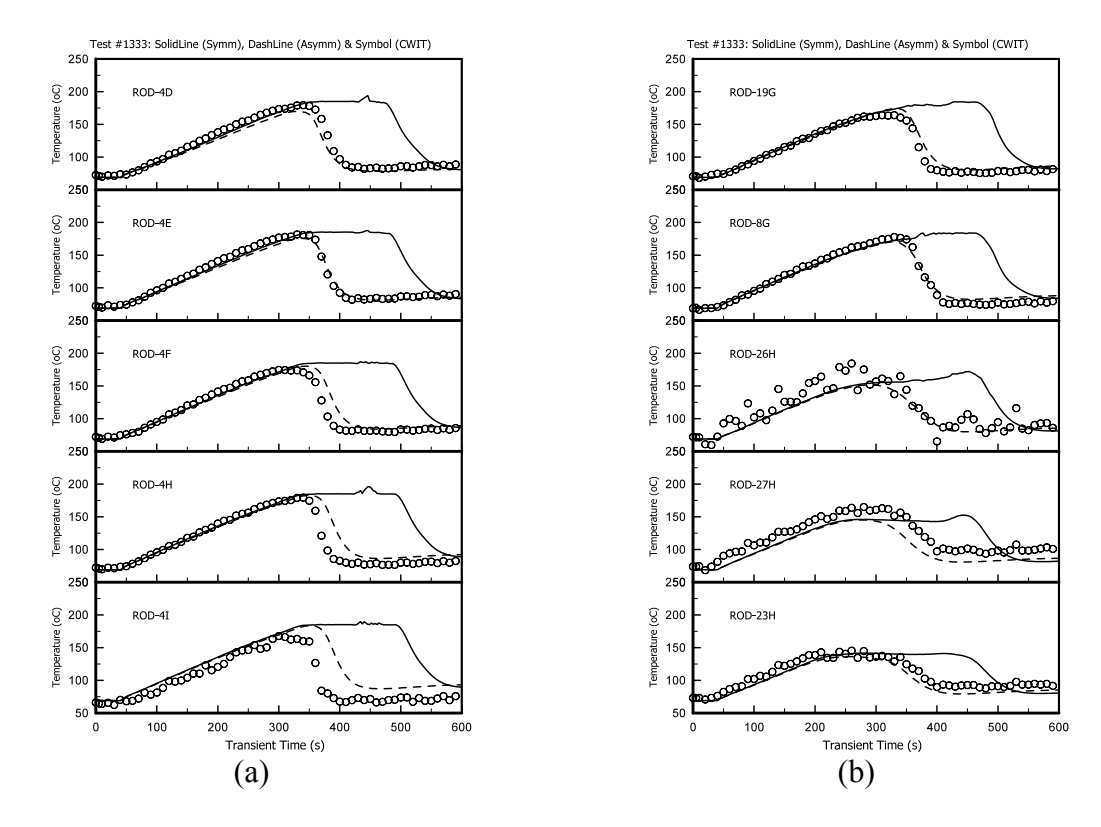
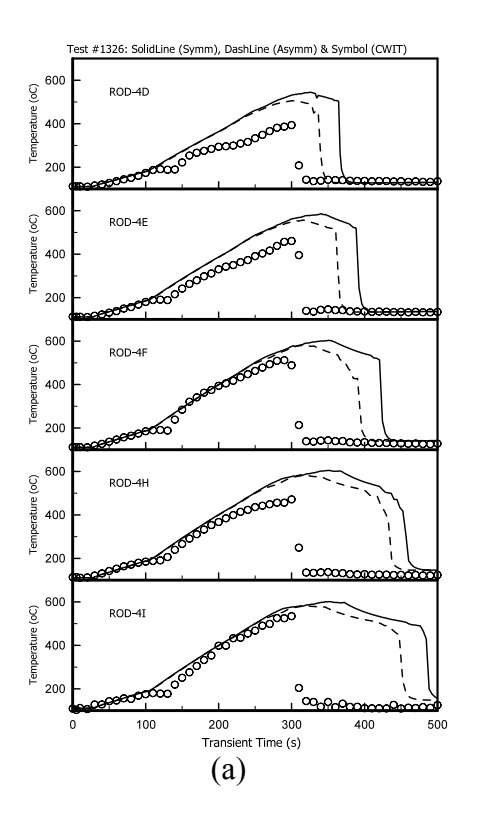


Figure 15 Comparisons of Rod-Surface Temperatures (Test #1333)



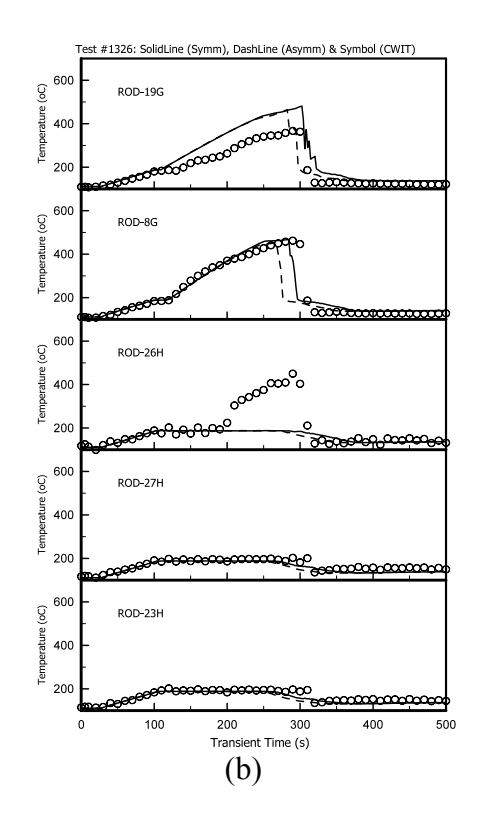
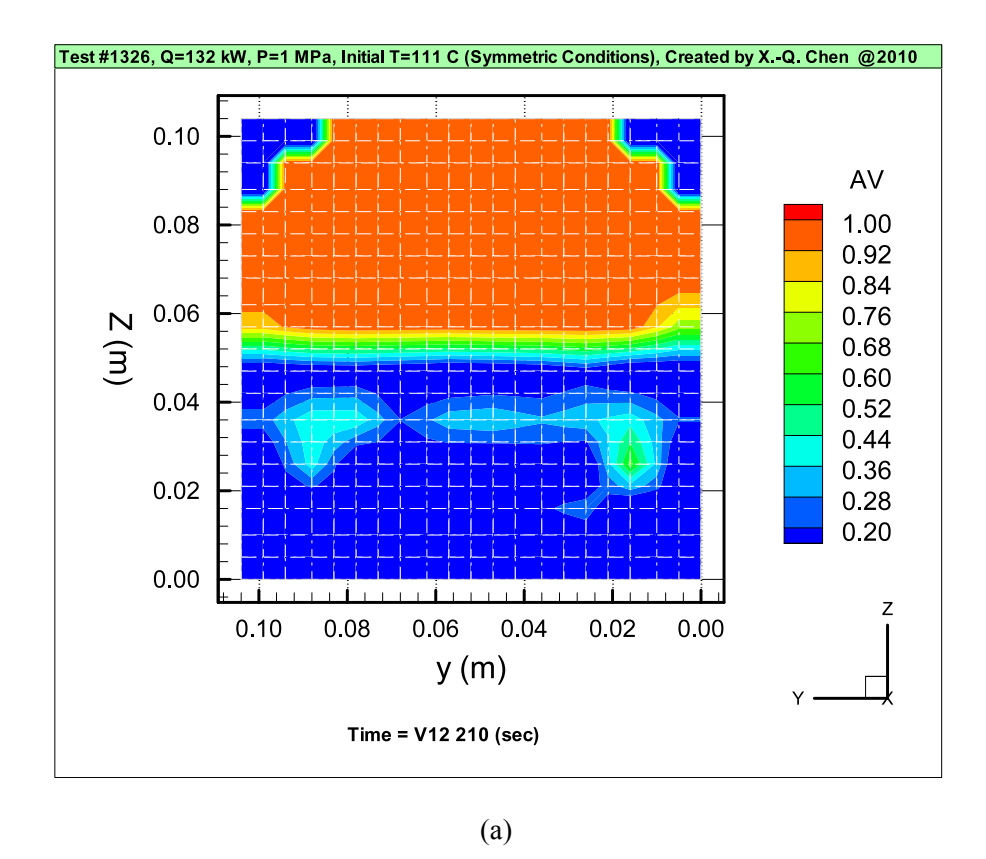


Figure 16 Comparisons of Pressure-Tube Surface Temperatures (Test #1326)



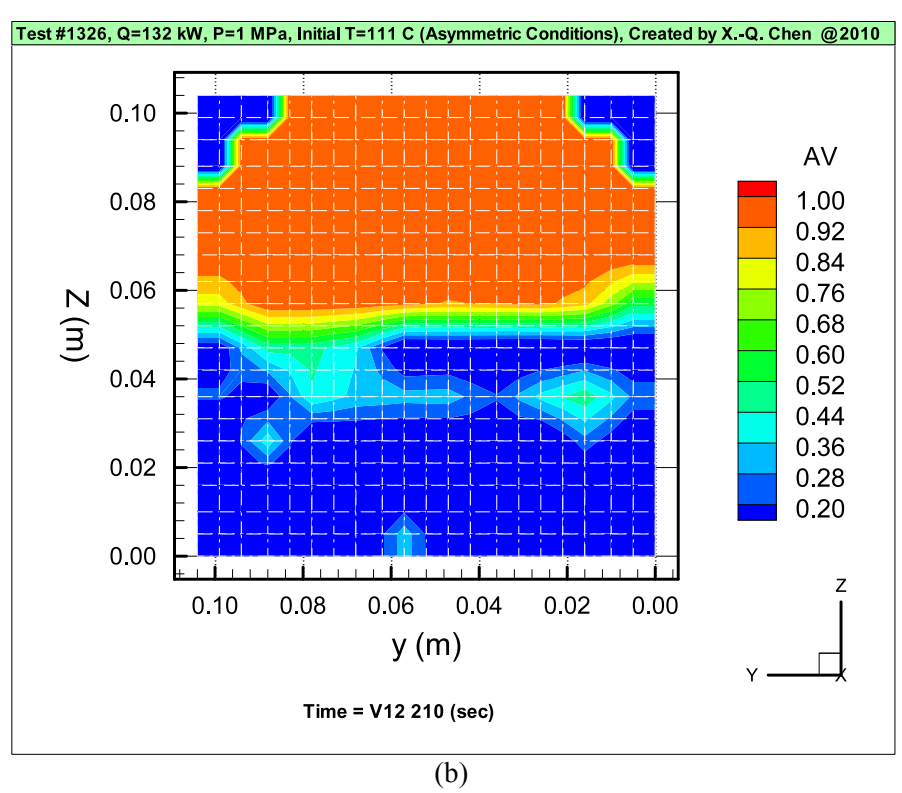


Figure 17 Contours of Steam Fractions at the Middle of Fuel Channel at 210s for Test #1326: (a) Symmetric and (b) Asymmetric

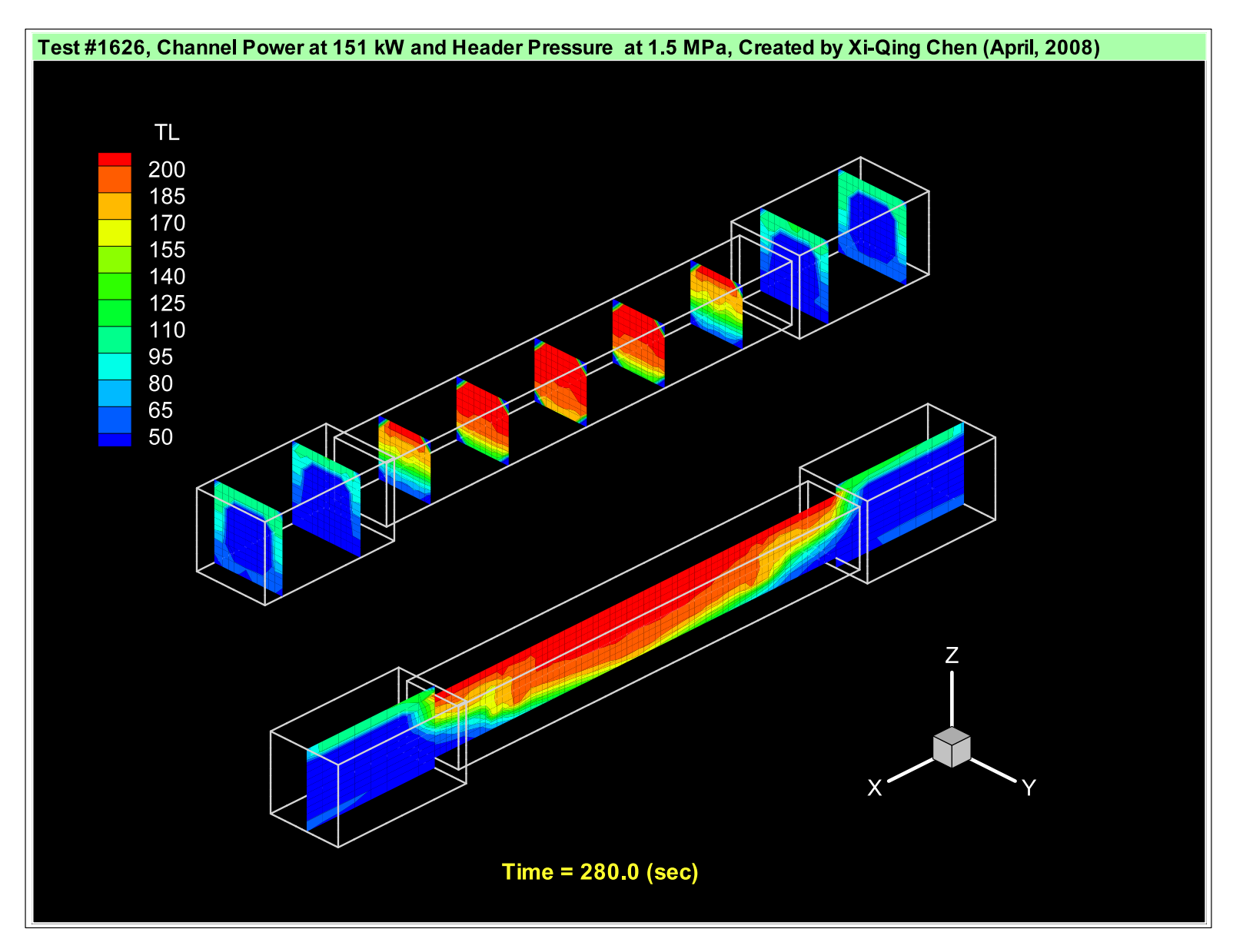


Figure 18 Contours of the Water Temperatures for Test #1626